

Accepted Manuscript

Research paper

Synthesis, crystal structures and antimicrobial activity of dimeric copper(II) complexes with 2-hydroxyphenyl-ethylidene-dithiocarbazates

Francielle C. Lima, Thayná S. Silva, Carlos H. G. Martins, Claudia C. Gatto

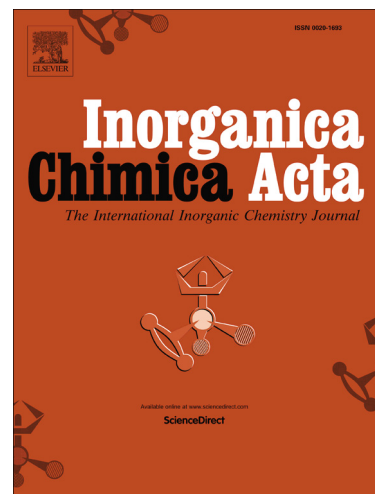
PII: S0020-1693(18)30832-6
DOI: <https://doi.org/10.1016/j.ica.2018.08.032>
Reference: ICA 18432

To appear in: *Inorganica Chimica Acta*

Received Date: 29 May 2018
Revised Date: 17 August 2018
Accepted Date: 22 August 2018

Please cite this article as: F.C. Lima, T.S. Silva, C. H. G. Martins, C.C. Gatto, Synthesis, crystal structures and antimicrobial activity of dimeric copper(II) complexes with 2-hydroxyphenyl-ethylidene-dithiocarbazates, *Inorganica Chimica Acta* (2018), doi: <https://doi.org/10.1016/j.ica.2018.08.032>

This is a PDF file of an unedited manuscript that has been accepted for publication. As a service to our customers we are providing this early version of the manuscript. The manuscript will undergo copyediting, typesetting, and review of the resulting proof before it is published in its final form. Please note that during the production process errors may be discovered which could affect the content, and all legal disclaimers that apply to the journal pertain.



**Synthesis, crystal structures and antimicrobial activity of
dimeric copper(II) complexes with 2-hydroxyphenyl-
ethylidene-dithiocarbazates**

Francielle C. Lima^a, Thayná S. Silva^b, Carlos H. G. Martins^b, Claudia C. Gatto^{a*}

^aLaboratory of Inorganic Synthesis and Crystallography, University of Brasilia (IQ-UnB). Campus Universitário Darcy Ribeiro, CEP 70904970, Brasília-DF, Brazil.

^bLaboratory of research in Applied Microbiology, University of Franca, CEP 14404-600, Franca-SP, Brazil.

* Corresponding author. Tel.: 55 61 31073872; fax: 55 61 31073900

E-mail address: ccgatto@gmail.com (C. C. Gatto)

ABSTRACT. The current work reports the synthesis and crystals structure of two copper(II) complexes $[(CuL^1)_2]$ (1) and $[(CuL^2)_2]$ (2), with *S*-allyl-2-(2-hydroxyphenyl-ethylidene)dithiocarbazato and *S*-benzyl-2-(2-hydroxyphenyl-ethylidene)dithiocarbazato (H_2L^1 and H_2L^2 , respectively). The single-crystal X-ray analyses reveal dimeric structures of the complexes with a distorted square planar coordination geometry. The phenoxo bridging mode observed in these complexes is located between the two copper atoms with *ONS*-donor ligands. The crystal packings are stabilized by hydrogen bonds involving the adjacent molecules. The compounds were also characterized by physicochemical and spectroscopic methods. The antibacterial and antifungal properties of the free dithiocarbazates and its Cu(II) complexes have been evaluated against several multiresistant bacteria and fungi. In all experiments, a superior antimicrobial activity of the complexes was observed compared to the free ligands.

KEYWORDS. Copper(II) complexes, dithiocarbazate, crystal structure, antimicrobial activity.

1. INTRODUCTION

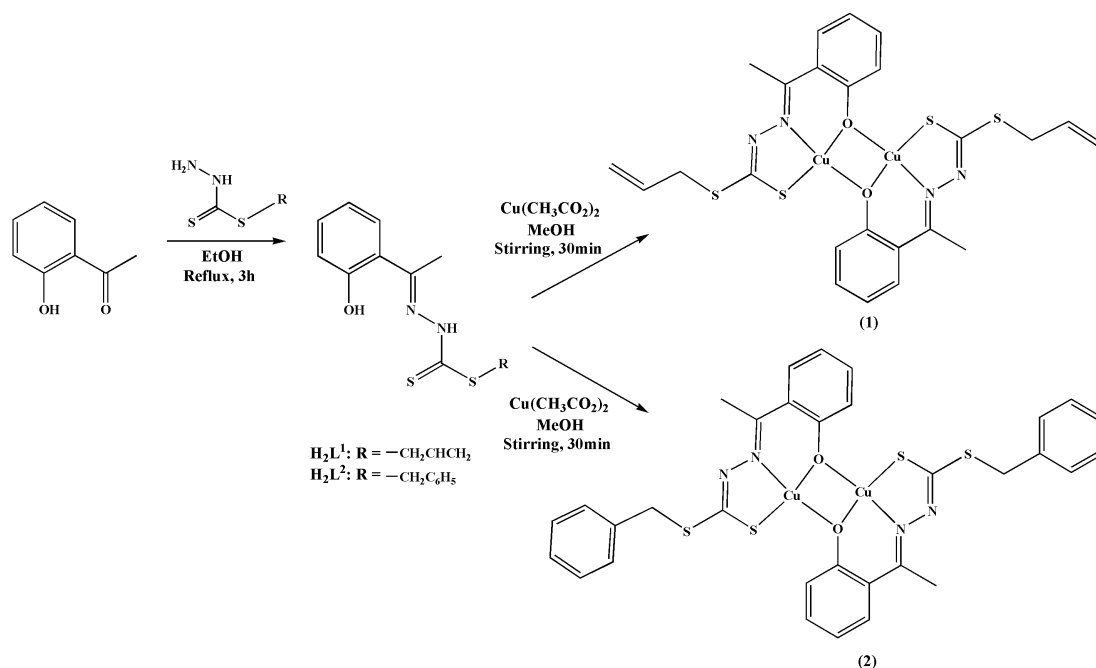
In recent years, there has been a rapid expansion in the investigation of metal-based antibacterial drugs, especially regarding the control of microbial proliferation, since it is considered the main cause of hospital complications, as well as nosocomial infections [1]. A variety of compounds has attracted great interest in the development of new compounds with biological activity, which are motivated by structural modifications caused by the coordination with metallic ions, targeting mechanisms of action that are more efficient and less toxic [2,3].

Transition metals possess special roles in biology, and copper is a trace metal essential to animals and plants. Actually, a variety of copper-based complexes have been investigated, mainly due to the therapeutic potential, which is increased by coordinating copper(II) complexes with mono- or polidentate Schiff bases chelates and donor atoms (N, O, S and halides) [4–6]. These derivatives from Cu(II) form stable compounds with a varied coordination number, from four to six, and the typical d^9 electronic configuration promotes $d-d$ transitions. In general, the activity of a metal complex depends of several factors, as the oxidation state, geometry, number and types of ligands [7–9].

Dithiocarbazates are Schiff bases with an increasing interest, particularly because of their properties that can be significantly modified by the introduction of different organic groups, providing a variety of donor properties relevant to coordination chemistry. In addition to this fact, the interaction of these donors with metallic ions, yields complexes with variable geometry and characteristics, and increases potential biological properties when compared to the free ligands [4,10,11]. In several cases, the activities of dithiocarbazate derivatives are very

different, although their structure may vary just slightly. In addition, since these ligands have both hard nitrogen atoms and soft sulfur donor atoms, they are able to coordinate with a wide range of metal ions, resulting in coordination compounds with intriguing physicochemical properties and potentiated biological applications [2,4].

Due to our interest in the study of new compounds with this type of ligand, we describe the synthesis, crystal structures, spectroscopy and biological activity of a new dithiocarbamate ligand and two new copper(II) complexes. The complexes $[(\text{CuL}^1)_2]$ (1) and $[(\text{CuL}^2)_2]$ (2) (where H_2L^1 and H_2L^2 are S-allyl-2-(2-hydroxyphenyl-ethylidene) dithiocarbamate and S-benzyl-2-(2-hydroxyphenyl-ethylidene) dithiocarbamate, respectively) were synthesized as Scheme 1, crystallized and analyzed using a single crystal X-ray diffraction. Moreover, a detailed assignment of IR, UV-vis of both the dithiocarbamates and their copper(II) complexes have been performed, as well NMR analysis of the ligands. The copper(II) complexes were evaluated against antimicrobial activity of multiresistant clinical isolates and certified microbial strains, and their biological response were compared with the free ligands.



Scheme 1. Synthesis of dithiocarbazates and their copper(II) complexes.

2. EXPERIMENTAL SECTION

2.1. Materials, methods, and instruments. The starting materials were obtained from a commercial source (Sigma-Aldrich) and used without further purification. The reagents and solvents were obtained from commercial sources. Elemental analyses were performed with Perkin Elmer/Series II 2400 analyzer. Fourier-transform infrared spectra were recorded from KBr pellets ($4000\text{-}400\text{ cm}^{-1}$) using an FT-IR Varian 640 spectrometer. UV-Vis spectra were collected on Varian-Cary and the concentration used for all analyses was $10\text{ }\mu\text{M}$ and $20\text{ }\mu\text{M}$. ^1H NMR and ^{13}C NMR analyses were conducted using an NMR YH 600 Oxford. The molar conductance of a 10^{-3} M solution of each metal complex in DMSO was measured at room temperature ($25\text{ }^\circ\text{C}$) using an Ion DDS 12DW microprocessor conductivity meter and a dip-type cell with a platinumized electrode.

2.2. Synthesis of the ligand S-allyl-2-(2-hydroxyphenyl-ethylidene) dithiocarbazato (H_2L^1). The mixture of 0.15 mL (3 mmol) hydrazine hydrate and 198 mg (3 mmol) KOH in 30 mL of ethanol was cooled down to 5° C. 0.180 mL (3 mmol) of carbon disulfide and 0.260 mL (1 mmol) of allyl bromide were added to the above mixture one by one with continuous stirring. After 1 h, 0.361 mL (3 mmol) of 2-hydroxyacetophenone was added and the mixture was refluxed and heated for 3 h. Yellow product was obtained and filtered off from the mother solution. Yield: 546 mg (70%). Melting Point: 116-118°C. Elemental analysis: calcd for $C_{12}H_{14}N_2S_2O$: C, 54.11; H, 5.28; N, 10.52 and found: C, 53.83; H, 5.14; N, 10.65. Selected IR bands (KBr, ν/cm^{-1}): $\nu(O-H)$, 3245; $\nu(N-H)$, 3184; $\nu(C=N)$, 1601; $\nu(C-O)$, 1219; $\nu(CSS)$, 1334; $\nu(C=S)$, 1101; $\nu(N-N)$, 936. UV-vis (DMF): $\lambda_{max} = 294$ and 361 nm; UV-vis (MeOH): $\lambda_{max} = 293$ and 358 nm. 1H NMR (DMSO- d_6) δ , ppm): 2.47 (s, 3H, CH_3), 3.90 (d, $^3J = 7.00$ Hz, 2H, S- CH_2), 5.34 and 5.17 (d, $^2J_{gem} = 1.10$ Hz, $^3J_{cis} = 9.90$ Hz, $^3J_{trans} = 16.87$ Hz, 2H, = CH_2), 5.88 (m, $^3J = 6.97$ Hz, $^3J_{cis} = 9.90$ Hz, $^3J_{trans} = 16.87$ Hz, H, - $CH=$), 7.64-6.93 (m, $^3J = 7.70$ Hz, H, Ar), 11.40 (s, H, Ar-O-H). ^{13}C NMR (DMSO- d_6) δ , ppm): 15.67 (CH_3), 40.13 (S- CH_2), 117.21 (= CH_2), 129.44 (- $CH=$), 118.83, 119.26, 119.75, 131.94, 132.62 (Ar), 157.44 (C_{Ar-OH}), 157.94 (C=N), 195.97 (C=S).

2.3. Synthesis of the S-benzyl-2-(2-hydroxyphenyl-ethylidene)dithiocarbazato (H_2L^2). The synthesis procedures for S-benzyl-2-(hydroxyphenyl-ethylidene) dithiocarbazate (H_2L^2) were followed according to a related methodology [12]. Melting Point: 145-147°C. Elemental analysis: calcd for $C_{16}H_{16}N_2S_2O$: C, 60.73; H, 5.10; N, 8.85 and found: C, 60.93; H, 5.55; N, 9.12. Selected IR bands (KBr, ν/cm^{-1}): $\nu(O-H)$, 3418; $\nu(N-H)$, 3179; $\nu(C=N)$, 1601; $\nu(C-O)$, 1228; $\nu(CSS)$, 1384; $\nu(C=S)$, 1057; $\nu(N-N)$, 948. UV-vis (DMF): $\lambda_{max} = 292$ and 376 nm; UV-vis (MeOH): $\lambda_{max} = 290$ and 348 nm.

2.4. Synthesis of (μ_2 -phenoxo) bis(S-allyl-2-(2-hydroxyphenyl-ethylidene)dithiocarbazato)-dicopper(II), [(CuL¹)₂] (1). H₂L¹ (31.60 mg, 0.1 mmol) was dissolved in 5 mL of methanol and added to a solution of Cu(CH₃COO)₂ (18.16 mg, 0.1 mmol) in 5 mL of methanol. The mixture was stirred for 30 min at room temperature. Dark green crystals, which were appropriate for X-ray diffraction, were filtered off from the mother solution. Yield: 379 mg (58 %). Melting Point: 187-189°C. Elemental analysis: calcd for C₂₄H₂₄N₄S₄O₂Cu₂: C, 43.95; H, 3.68; N, 8.54 and found: C, 44.34; H, 3.82; N, 8.94. Selected IR bands (KBr, ν/cm^{-1}): $\nu(\text{C}=\text{N})$, 1593; $\nu(\text{C}-\text{O})$, 1159; $\nu(\text{CSS})$, 1300; $\nu(\text{N}-\text{N})$, 1003. UV-vis (DMF): $\lambda_{\text{max}} = 324$ and 405 nm; UV-vis (MeOH): $\lambda_{\text{max}} = 322$ and 382 nm. Molar conductivity (10^{-3} mol.L⁻¹, DMSO): 9.92 Ω^{-1} cm² mol⁻¹.

2.5. Synthesis of (μ_2 -phenoxo) bis(S-benzyl-2-(2-hydroxyphenyl-ethylidene)dithiocarbazato)-dicopper(II), [(CuL²)₂] (2). H₂L² (24 mg, 0.1 mmol) was dissolved in 5 mL of methanol and added to a solution of Cu(CH₃COO)₂ (18.16 mg, 0.1 mmol) in 5 mL of methanol. The mixture was stirred for 30 min at room temperature. Dark green crystals, which were appropriate for X-ray diffraction, were obtained directly from the mother liquor upon standing the solution at room temperature for several days. Yield: 475 mg (63 %). Melting Point: 183-185°C. Elemental analysis: calcd for C₃₂H₂₈N₄S₄O₂Cu₂: C, 50.84; H, 3.73; N, 7.41 and found: C, 50.36; H, 3.46; N, 7.46. Selected IR bands (KBr, ν/cm^{-1}): $\nu(\text{C}=\text{N})$, 1597; $\nu(\text{C}-\text{O})$, 1226; $\nu(\text{CSS})$, 1296; $\nu(\text{N}-\text{N})$, 1004. UV-vis (DMF): $\lambda_{\text{max}} = 324$ and 395 nm; UV-vis (MeOH): $\lambda_{\text{max}} = 322$ and 380 nm. Molar conductivity (10^{-3} mol.L⁻¹, DMSO): 28.40 Ω^{-1} cm² mol⁻¹.

2.6. Crystal structure determination. The X-ray diffraction data were collected on a Bruker CCD SMART APEX II single crystal diffractometer with Mo K α radiation

(0.71073 Å). SADABS [13] was used to scale the data and perform the multi-scan absorption correction. The structures were solved by direct methods using SHELXS-97 [14] and subsequent Fourier-difference map analyses yielded the positions of the non-hydrogens atoms, the refinement was performed using SHELXL-2018 [15]. Molecular graphics were generated with POV-Ray [16] and DIAMOND [17] programs. The crystal data, experimental details and refinement results are summarized in Table 1.

2.7. Antibacterial assay.

2.7.1. Bacterial strains. To evaluate the antibacterial activity of the free ligands and copper(II) derivatives, multiresistant clinical isolates and bacterial strains from the American Type Culture Collection (ATCC) and National Collection of Type Cultures (NCTC) were employed, namely: *Staphylococcus epidermidis* (isolated from blood); *S. epidermidis* (ATCC 14990); *Staphylococcus capitis* (ATCC 27840); *Enterococcus faecalis* (isolated from urine); *E. faecalis* (NCTC 775); *Staphylococcus aureus* (isolated from surgical wound), *S. aureus* (ATCC 29213); *Pseudomonas aeruginosa* (isolated from urine); *Klebsiella pneumoniae* (isolated from urine); *Enterococcus faecium* (NCTC 7171); and *Enterobacter cloacae* (isolated from hospital outbreak). The multiresistant clinical isolates were kindly supplied by Hospital das Clínicas de Ribeirão Preto (São Paulo State, Brazil).

2.7.2. Determination of the Minimum Inhibitory Concentration. The Minimum Inhibitory Concentration (MIC) values corresponds to the minimum concentration of sample that is able to inhibit the growth of microorganisms, and were determined by the microdilution broth method in 96-well microplates, in triplicate [18]. The samples were dissolved in dimethylsulfoxide (DMSO, Sigma-Aldrich) at 1.0 $\mu\text{g mL}^{-1}$, followed by

dilution in cation-adjusted Mueller-Hinton broth – (Difco, Kansas City, MO, USA); until concentrations ranging from 400.0 to 0.195 $\mu\text{g mL}^{-1}$ were achieved. The final DMSO content was 5% (v/v). The inoculum was adjusted for each organism, to yield a cell concentration of 5×10^5 colony forming units (CFU) per mL, according to guidelines of the Clinical and Laboratory Standards Institute[18]. DMSO 5% (v/v) was used as negative control; to validate the tests, the positive control tetracycline was tested against reference strains of *S. aureus* (ATCC 29213) and *Escherichia coli* (ATCC 25922) [18] in a range of MIC values between 0.0115 and 5.9 $\mu\text{g mL}^{-1}$. One inoculated well was included, to control broth adequacy for bacterium growth. Another well containing broth free of antimicrobial agent and inoculum was included, to control medium sterility. The microplates (96 wells) were incubated for 24 h at 37° C. After the incubation period, 30 μL of resazurin aqueous solution (0.02%) was added to the microplates [19], for observation of bacterial growth: the blue and red color indicated absence and presence of bacterial growth, respectively. The microplates were re-incubated for 30 min and observed and analyzed in a descriptive way [19]. All assays were carried out in triplicate.

2.7.3. Antifungal activity against *Candida* spp. The microorganism tested were *Candida albicans* (ATCC 28366), *C. tropicalis* (ATCC 13803) and *C. glabrata* (ATCC 15126), from American Type Culture Collection (ATCC). The assays were performed using method of broth microdilution using the standards recommended by Clinical and Laboratory Standards Institute.[20] The stock solutions were prepared by dissolving the samples, in DMSO (Sigma-Aldrich) in a concentration of 192,000 $\mu\text{g mL}^{-1}$. Dilutions with stock solutions were made using the standard RPMI 1640 medium buffered to pH 7.2 with 0.165 mol L^{-1} of 3-N-morpholinepropanesulfonic acid (MOPS, Acros Organics, Geel, Turnhout, Belgium) of 12,000 $\mu\text{g mL}^{-1}$. The inoculum was prepared

using a spectrophotometric method (at 530 nm wavelength), and compared with a 0.5 McFarland scale to obtain the value of 6.0×10^6 CFU mL⁻¹. Then, the dilutions recommended by CLSI with RPMI until the inoculums reached 1.2×10^3 UFC mL⁻¹.

The MIC values were also evaluated for these microorganisms and all assays were carried out in triplicate. It was performed using 96-well microplates, where series of dilutions with final concentrations were made in the range of 1.46 to 3,000.0 µg mL⁻¹. Each well received 100.0 µL of the inoculum suspension and the final volume in each well was 200.0 µL. The negative control (DMSO) was tested with concentrations ranging from 1% to 10% v/v and not influenced in yeast growth. The added inoculum medium was used as culture growth control. To validate the tests, amphotericin B (positive control) was tested against reference strains of *C. krusei* (ATCC 6258) and *C. parapsilosis* (ATCC 22019) in a range of MIC values between 0.031 and 16.0 µg mL⁻¹. If the MIC value is within this range for these yeasts, the methodology and the results for the other tested yeasts are validated according to the reference protocol M27-A3.[20] At the end of the procedure, after incubation, 30 µL of a 0.02% aqueous resazurin (Sigma) solution was added to each well and the microplates were incubated for further 30 min. For observation and descriptive analysis, the blue and red colors represent the absence and the presence of microbial growth, respectively [21].

(Table 1)

3. RESULTS AND DISCUSSION

3.1. Synthesis and Crystal Structure Description

Two tridentate *ONS* - ligands were synthesized by the condensation reaction of 2-hydroxyacetophenone with *S*-allyldithiocarbamate and *S*-phenyldithiocarbamate.

Each ligand reacted separately with $\text{Cu}(\text{CH}_3\text{COO})_2$ at methanol solution. These compounds were characterized by elemental analysis and spectroscopic techniques. These results supported the structures obtained by single crystal X-ray in which H_2L^1 and H_2L^2 behaved as tridentate donor ligands coordinating via the phenolic oxygen, azomethine nitrogen and thione sulfur atom.

The crystal structure of H_2L^1 is established accurately by single-crystal X-ray diffraction (Figure 1), whereas crystal structure of H_2L^2 ligand has already been elucidated by Biswal et al. 2015 [12]. These ligands can exhibit thione-thiol tautomerism in the $-\text{HN}-\text{C}=\text{S}$ functional group; however, the ^1H NMR spectra does not show any peak attributable to the $\text{S}-\text{H}$ proton and the IR spectra show the $\nu(\text{C}=\text{S})$ band around 1100 cm^{-1} , suggesting the presence of the thione form in solution and in the solid state. The thione form is also predominant in solution in the presence of metal ions and soft bases, in order to favor the coordination with the metal ion. The thione tautomer is confirmed both by the presence of the hydrazinic hydrogen and the characteristic double distance $\text{C}(9)-\text{S}(1)$ of $1.659(2)\text{ \AA}$ [22]. The ligand adopts an *E* configuration with respect to the $\text{C}(7)-\text{N}(1)$ and *Z* configuration with respect to the $\text{N}(2)-\text{C}(9)$ bond, and the entire species has coplanar atoms, with the exception of the atoms of the final portion of the ligand, due the greater liberty, how found in others similar dithiocarbazates and thiosemicarbazones [23–27]. The displacement to greater lengths of the bonds $\text{C}(9)-\text{N}(2)$ of $1.353(3)\text{ \AA}$ and $\text{C}(8)-\text{S}(2)$ of $1.734(2)\text{ \AA}$ and shorter for $\text{N}(1)-\text{N}(2)$ of $1.372(3)\text{ \AA}$, are indicative of the delocalization of electrons through the dithiocarbazate function by virtue of the coordination with the metal center. The $\text{N}-\text{N}$ and $\text{C}-\text{N}$ bond lengths of the dithiocarbazate moiety are comparable to the corresponding lengths of other similar compounds [26,28]. The bond length

C(1)–O(1) of 1.354(3) Å corresponds to a single bond C–O, evidencing the protonated form of the hydroxyl as a free ligand [12,24]. Selected bond lengths and bond angles are given in Table 2.

(Figure 1)

Interestingly, the phenolic oxygen atom can form a bifurcated intramolecular hydrogen bonds with the azomethine nitrogen atom and the thioether sulfur atom. This interaction between O(1)–H(1)⋯N(1) [$d(\text{O}\cdots\text{N}) = 2.588(3)$ Å, $\angle(\text{O}(1)\text{H}(1)\cdots\text{N}(1)) = 152^\circ$] and O(1)–H(1)⋯S(2) [$d(\text{O}\cdots\text{S}) = 3.375(2)$ Å, $\angle(\text{O}(1)\text{H}(1)\cdots\text{S}(2)) = 138^\circ$], possesses a significant role in the structural arrangement of the ligand, stabilizing its structure by forming five/six membered rings [29,30]. Additionally, an intermolecular hydrogen bond is observed in the crystal lattices, N(2)–H(2A)⋯S(1)^a [$d(\text{N}\cdots\text{S}) = 3.580(2)$ Å, $\angle(\text{N}(2)\text{H}(2\text{A})\cdots\text{S}(1)) = 173^\circ$ with symmetry operator (^a): $-x+1, -y+2, -z$], different from reported by Zangrando et al. 2015 [10] and Takjoo and Centore 2013 [24] with the formation of a polymer obtained by the repetition of linear chains of similar ligands.

The crystal structure determination (1) with H₂L¹ and (2) with H₂L² revealed a dinuclear centrosymmetric copper(II) complexes. The anisotropic thermal displacement ellipsoids representations of the complexes are illustrated in Figure 1. The bond lengths and angles (listed in Table 2) are in good agreement with those reported for other copper(II) dithiocarbazate complexes.

(Figure 2)

In the two complexes, the dithiocarbazates H₂L¹ and H₂L² acts as doubly deprotonated ligands, coordinated in the *E* isomer form, with respect to the N(2)–

C(9), which chelates the copper(II) atom through the phenoxo oxygen O(1), the imine nitrogen N(1) and thiol sulfur S(2) atoms [23,25,26]. The metal centers exhibits a square planar geometry and an interesting feature of the compounds is that the organic ligands act as bridges μ_2 -phenoxo between two copper atoms in a fashion that one 5-membered and one 6-membered rings are established. The oxygen atoms of the phenolate groups form a planar central $\{\text{Cu}_2\text{O}_2\}$ ring. Thus, the formation of an oxygen bridge between two copper atoms does not result in a significant lengthening of the corresponding Cu–O bonds that are between 1.908(18) and 2.005(3) Å. The bonding mode results in a Cu–Cu' distances of 2.926(6) Å for (1) and 2.966(10) Å for (2), which are similar to the values observed in hydroxo-bridged dimers [31–34].

For both complexes, the coordination environment around the central Cu(II) atom is best described as tetracoordinated in bonds of atoms O(1), N(1), S(2) and O(1)', resulting in the distorted square planar geometry. The bond angles O(1)–Cu1–N(1), N(1)–Cu1–S(1), S(1)–Cu1–O(1)', O(1)'–Cu1–O(1), differ from 90°, as well, the bond angles O(1)–Cu1–S(1), N(1)–Cu1–O(1)', which differ from 180°, as it is expected for a perfect geometry [23,30,31]. The distorted geometry can be explained by the rigidity of the ligands and additionally, by the manner in which the ligands behave around the central atom, with bridged dimers configuration. The angles between neighboring donor atoms in the chelates rings are between 88.62(11)° and 93.73(13)° and O(1)–Cu1–O(1)' of 76.60(9)° for (1) and 76.67(12)° for (2).

(Table 2)

There are slight changes in the bonding lengths for the ligands after their coordination to the metal center. The bond length C(9)–S(1) increases from 1.659(2) Å for H₂L¹ to 1.728(3) Å for (1) and 1.661(3) Å for (H₂L²) [12] to 1.728(4) Å for (2), evidencing the coordination of the metal on that site [23]. Commonly, the related complexes have their ligands coordinated in their tautomeric form, a deprotonated thiolate, as already observed for most of the S-alkyl/aryl dithiocarbamate derivative compounds. In the same way, C(9)–N(2) suffers a significant decrease from 1.353(3) Å for H₂L¹ to 1.284(3) Å for the complex (1) and of 1.352(3) Å for the ligand (H₂L²) [12] to 1.284(3) Å for the complex (2), suggesting a resonance of the electric charge due to the complexation of the adjacent coordination sites [23]. Considering the structural similarity of the two complexes, the bond lengths involving the coordination polyhedron for the copper atoms are in agreement with previous literature studies and are evidenced by the bond lengths Cu(1)–N(1) of 1.940(2) Å for (1) and 1.935(3) Å for (2), as well as, Cu(1)–S(1) of 2.199(3) Å for (1) and 2.201(13) Å for (2)[12,23].

3.2. Spectroscopic Analyses. FT-IR spectra of (1) and (2) were compared with the free dithiocarbamates. The bands attributed to of $\nu(\text{OH})$ vibration appear around 3245 cm⁻¹ for H₂L¹ and 3418 cm⁻¹ for H₂L², while $\nu(\text{NH})$ are attributed in 3184 cm⁻¹ for H₂L¹ and 3179 cm⁻¹ for H₂L². These bands disappear with coordination to the copper atoms and shows the coordination of dithiocarbamate through the phenoxo oxygen and the imine nitrogen [10,24,35]. Additionally, the presence of a band $\nu(\text{C}=\text{S})$ absorption at 1101 cm⁻¹ and 1057 cm⁻¹ for H₂L¹ and H₂L², respectively, are not observed in the spectra of the complexes, indicating an electronic delocalization of the ligands during complexation [25].

In the spectra of the free dithiocarbazates one peak was observed at 1601 cm^{-1} , which can be attributed to $\nu(\text{C}=\text{N})$ and the metal complexes (1) and (2) exhibited a $\nu(\text{C}=\text{N})$ absorption at 1593 cm^{-1} and 1597 cm^{-1} , respectively [29,35,36]. The band shift attributed to $\nu(\text{C}=\text{N})$ was lower for the complexes when compared to the free ligand, indicating the electronic delocalization along the structure as soon as N(2) was coordinated to the copper centers. In the IR spectra of the complexes (1) and (2), a band $\nu(\text{C}-\text{N})$ were observed at 1468 cm^{-1} and 1568 cm^{-1} , respectively [25]. In the complexes, the bands observed at 1003 cm^{-1} for (1) and 1004 cm^{-1} for (2) are assigned to a $\nu(\text{N}-\text{N})$. Therefore, the IR data for the complexes indicate a coordination of the dithiocarbazate ligands through the *ONS*-donor atoms, in accordance with the crystal structures determination.

The UV-Vis experiment was made at room temperature, using two different solvents (MeOH and DMF), for organic ligands and copper complexes (Figure 3). The results are summarized in Table 3. Regardless of the solvent, all compounds spectra presented $\pi-\pi^*$ and $n-\pi^*$ bands correspondent to the transitions of the dithiocarbazate moiety, as well as the $\pi-\pi^*$ transition, characteristic of the azomethine chromophore, for which the metallic complexes presents a hypochromic displacement attributed to the coordination of the copper atom to azomethine nitrogen [10,24,25]. The transitions in the median region of the spectra (300-400 nm) correspond to the ligand-metal charge transitions of the complexes as well as the transitions in the ultraviolet region are between the orbitals of the metal. The presence of a discrete signal at $265\text{ nm H}_2\text{L}^1$ and $264\text{ nm H}_2\text{L}^2$ refers to the $\pi-\pi^*$ transition of the aromatic ring, while the strong absorption bands in the range of 358-376 nm are presumably attributed from the occurrence of $\pi-\pi^*$ and $n-\pi^*$ transitions of the characteristic moiety of the dithiocarbazate ligand itself, the band being present in the 290-293 nm range attributed to the $\pi-\pi^*$ transition of the

chromophore azomethine of the obtained Schiff base [10,26]. As already predicted, the mentioned transitions in the complexes presented lower wavelengths, partially due to the strong nitrogen absorption of the azomethine fragment, being evidenced at 287–289 nm and 322–324 nm. Additionally, the bands in the lower energy region, 380–405 nm, for both complexes, are attributed to the charge transfer $S \rightarrow M$ (II) (LMCT), affording one more evidence of coordination by this sites to the metallic center [10]. The band at 583 nm for (1) and 580 nm for (2) are related to the d–d transition of the metal ions, being the predicted ${}^2A_1 \rightarrow {}^2B_1$ spectroscopic term agreeing with a square planar geometry [10,24]. In addition, the UV-vis of (1) and (2) was evaluated at different times (see Supporting Information, Figure S1). Over time, the characteristic absorption of each complex displayed no significant change in the absorption bands. The results of UV-vis spectra analysis reveal that (1) and (2) are stable in solution in a 72 h period, indicating no dissociation in the room temperature.

(Figure 3)

(Table 3)

The ${}^1\text{H}$ NMR spectra of the ligand in DMSO- d_6 displays the presence of an unshielded signal at 11.40 ppm, ascribed to the –NH resonance of the thioamide function of the ligand. The methylene protons (–CH₂) of the dithiocarbazate moiety appears as a doublet (d) (${}^3J = 7$) with an integrated value of 2 at 3.90 ppm. The protons –CH₂ and –CH of the allyl group present multiple signals at 5.34–5.37 (dd) (${}^2J_{\text{gem}} = 1.10$ Hz and ${}^3J_{\text{trans}} = 16.87$ Hz), 5.17–5.19 (dd) (${}^2J_{\text{gem}} = 1.10$ Hz and ${}^3J_{\text{cis}} = 9.90$ Hz) and 5.88–5.95 ppm (m) (${}^3J = 6.97$ Hz, ${}^3J_{\text{cis}} = 9.90$ Hz and ${}^3J_{\text{trans}} = 16.87$ Hz), respectively [23]. A single signal for methyl appears in the most shielded region at 2.47 ppm [26]. The aromatic protons appear as doublets and double doublets in the range of 6.93–7.64

ppm ($^3J = 7.70$) [37]. Due to the higher acidity and, consequently, hydroxyl proton lability, it was not possible to measure its resonance signal.

The ^{13}C NMR spectra shows twelve signals for the ligand, the main ones being characterized in the most unshielded region of the spectra, where it is possible to assign the signals of the carbon bonded to sulfur of the thione ($\text{C}=\text{S}$) function in 195.47 ppm, the carbon of the azomethine ($\text{C}=\text{N}$) in 157.98 ppm, $\text{C}-\text{O}$ at 157.44 ppm. The moiety of allyl substituent, methylene, $-\text{CH}=\text{e}=\text{CH}_2$ are characterized in 40.13, 117.21 and 129.44 ppm, which are in agreement with the literature [24,26].

The molar conductances of 10^{-3} M solutions of the compounds in DMSO are in the range $9.92\text{--}28.40 \Omega^{-1} \text{ cm}^2 \text{ mol}^{-1}$ therefore the complexes behave as non-electrolytes in DMSO, since the measured conductivities are below the limit proposed by Geary [38] of $35 \Omega^{-1} \text{ cm}^2 \text{ mol}^{-1}$ for non-electrolytic species. It can be concluded, therefore, that the ligands are tightly bound to the metal center.

3.3. Biological activity. According to our interest, the biological activity of the synthesized compounds was tested against Gram-negative bacteria, Gram-positive and fungi. The results for the tests were expressed by the minimal inhibitory concentration (MIC) according to Tables 4 and 5, through which it evaluates the lowest concentration ($\mu\text{g.mL}^{-1}$) capable of inhibiting microbial growth.

With the exception of the strains *P. aeruginosa*, *E. cloacae*, *E. faecalis* and *S. aureus* that did not present any satisfactory response, the inhibitory activity of the complexes was superior compared to the ligands. The complexes manifested considerable antimicrobial activity to *S. aureus* (MIC = $1.56 \mu\text{g.mL}^{-1}$ of (1) and $3.12 \mu\text{g.mL}^{-1}$ of (2)), *S. capitis* (MIC = $3.12 \mu\text{g.mL}^{-1}$ of (1) and $6.25 \mu\text{g.mL}^{-1}$ of (2)) and *S. epidermidis* (MIC = $3.12 \mu\text{g.mL}^{-1}$ of (1) and $6.25 \mu\text{g.mL}^{-1}$ of (2)). The

antifungal tests followed the same tendency in which the complexes presented higher activity when compared to the ligands, *C. glabrata* (MIC = 375 $\mu\text{g}\cdot\text{mL}^{-1}$ of (1) and 375 $\mu\text{g}\cdot\text{mL}^{-1}$ of (2)), *C. tropicalis* (MIC = 375 $\mu\text{g}\cdot\text{mL}^{-1}$ of (1) and 750 $\mu\text{g}\cdot\text{mL}^{-1}$ of (2)) and *C. albicans* (MIC = 1500 $\mu\text{g}\cdot\text{mL}^{-1}$ of (1) and 750 $\mu\text{g}\cdot\text{mL}^{-1}$ of (2)).

Moreover, the results evidently show that the antimicrobial activity of the metal ion became more pronounced when coordinated to the dithiocarbazate derivatives. The complexation of dithiocarbazates with metal ions reduces its polarity by partially sharing the positive charge with the donor atoms and π -electron delocalization, and this can result in an improvement of the lipophilic characteristics of the metallic atom, improving the activity of the compounds, since it allows, in part, the blocking of cellular enzymatic activity [37,39]. Additionally, the compounds showed greater activity against Gram-positive bacteria according the tendency of most reports [2,5,40]. In general, compounds (1) and (2) presented superior activity for all the evaluated assays, a result that can be attributed mainly to the presence of the metal coordination, which contributes to the antibiotic activity.

(Table 4)

(Table 5)

4. CONCLUSIONS

In this paper, we have described the synthesis and crystal structure of a new ligand and two stable copper(II) complexes of dithiocarbazate derivatives. Both X-ray crystal analysis and the spectral characterization of the H_2L^1 ligand ratify its structure in a

thione tautomer with bifurcated intramolecular hydrogen bonds. The dithiocarbazates are doubly-deprotonated and tridentate coordinated to copper(II) atoms in the formation of the dimeric complexes. The biological analyses show satisfactory results of the copper complexes, with positive response of microbiological assay and greater activity against Gram-positive bacteria. The successful synthesis and characterization and the promising results against the antibacterial agents of copper(II) complexes with dithiocarbazates constitute a starting point to the development of new compounds and their applications as promising antimicrobial agents.

ASSOCIATED CONTENT

Supporting Information

Crystallographic data for the structures in this work have been deposited to the Cambridge Crystallographic Data Centre, CCDC 1822218-1822220. Copies of the available material can be obtained free of charge by application to the Director, CCDC, 12 Union Road, Cambridge CH2 1EZ, UK (Fax: +44 1223 336033; E-mail: deposit@ccdc.cam.ac.uk or <http://www.ccdc.cam.ac.uk>). Supplementary tables, figures, NMR and IR spectra are as detailed in the text (PDF). Crystallographic data are in CIF files.

AUTHOR INFORMATION

Corresponding Authors

*E-mail for Claudia C. Gatto: ccgatto@gmail.com

Author Contributions

The manuscript was written with contributions from all authors. All authors have approved the final version of the manuscript.

Funding Sources

This work has been partially supported by FAPDF, FINEP/CTINFRA, CNPq, CAPES, FINATEC and DPG-UnB. The authors wish to thank FAPESP (process number 2015/23850-5).

ACKNOWLEDGMENTS

All funding agencies are acknowledged for partial financial support.

REFERENCES

- [1] M. Akbar Ali, A.H. Mirza, R.J. Butcher, M.T.H. Tarafder, M.A. Ali, Synthetic, spectroscopic, biological and X-ray crystallographic structural studies on a novel pyridine-nitrogen-bridged dimeric nickel(II) complex of a pentadentate N3S2 ligand, *Inorganica Chim. Acta.* 320 (2001) 1–6.
doi:[https://doi.org/10.1016/S0020-1693\(01\)00452-2](https://doi.org/10.1016/S0020-1693(01)00452-2).
- [2] M.L. Low, L. Maigre, P. Dorlet, R. Guillot, J.-M. Pagès, K.A. Crouse, C. Policar, N. Delsuc, Conjugation of a New Series of Dithiocarbamate Schiff Base Copper(II) Complexes with Vectors Selected to Enhance Antibacterial Activity, *Bioconjug. Chem.* 25 (2014) 2269–2284. doi:10.1021/bc5004907.
- [3] R.J. Fair, Y. Tor, Antibiotics and Bacterial Resistance in the 21st Century, *Perspect. Medicin. Chem.* 6 (2014) PMC.S14459. doi:10.4137/PMC.S14459.
- [4] M. Kudrat-E-Zahan, M.S. Islam, Synthesis, characterization, and antimicrobial activity of complexes of Cu(II), Ni(II), Zn(II), Pb(II), Co(II), Mn(II), and U(VI) containing bidentate Schiff base of [S-methyl-3-(4-

- methoxybenzylidene)dithiocarbazate], *Russ. J. Gen. Chem.* 85 (2015) 979–983.
doi:10.1134/S1070363215040350.
- [5] M.L. Low, G. Paulus, P. Dorlet, R. Guillot, R. Rosli, N. Delsuc, K.A. Crouse, C. Policar, Synthesis, characterization and biological activity of Cu(II), Zn(II) and Re(I) complexes derived from S-benzylidithiocarbazate and 3-acetylcoumarin, *BioMetals*. 28 (2015) 553–566. doi:10.1007/s10534-015-9831-2.
- [6] C. Duncan, A.R. White, Copper complexes as therapeutic agents, *Metallomics*. 4 (2012) 127–138. doi:10.1039/C2MT00174H.
- [7] S.T. and L. Marchio, Copper Compounds in Anticancer Strategies, *Curr. Med. Chem.* 16 (2009) 1325–1348.
doi:http://dx.doi.org/10.2174/092986709787846532.
- [8] D. Denoyer, S. Masaldan, S. La Fontaine, M.A. Cater, Targeting copper in cancer therapy: “Copper That Cancer,” *Metallomics*. 7 (2015) 1459–1476.
doi:10.1039/C5MT00149H.
- [9] C. Santini, M. Pellei, V. Gandin, M. Porchia, F. Tisato, C. Marzano, Advances in Copper Complexes as Anticancer Agents, *Chem. Rev.* 114 (2014) 815–862.
doi:10.1021/cr400135x.
- [10] E. Zangrando, M.T. Islam, M.A.-A.A.A. Islam, M.C. Sheikh, M.T.H. Tarafder, R. Miyatake, R. Zahan, M.A. Hossain, Synthesis, characterization and bio-activity of nickel(II) and copper(II) complexes of a bidentate NS Schiff base of S-benzyl dithiocarbazate, *Inorganica Chim. Acta*. 427 (2015) 278–284.
doi:https://doi.org/10.1016/j.ica.2014.12.014.
- [11] A.H. Mirza, M. Akbar Ali, P. V Bernhardt, I. Asri, Dimeric nickel(II) and copper(II) complexes of the pentadentate N3S2 chelating agents derived from S-alkyl/aryl esters of dithiocarbazic acid, *Polyhedron*. 81 (2014) 723–727.

- doi:<https://doi.org/10.1016/j.poly.2014.07.033>.
- [12] D. Biswal, N.R. Pramanik, S. Chakrabarti, N. Chakraborty, K. Acharya, S.S. Mandal, S. Ghosh, M.G.B. Drew, T.K. Mondal, S. Biswas, Lewis base controlled supramolecular architectures via non-covalent interactions of dioxomolybdenum(vi) complexes with an ONS donor ligand: DFT calculations and biological study, *New J. Chem.* 39 (2015) 2778–2794. doi:10.1039/C4NJ02225D.
- [13] G.M. Sheldrick, SADABS, Program for Empirical Absorption Correction of Area Detector Data: University of Göttingen: Germany, (1997).
- [14] G.M. Sheldrick, SHELXS-97. Program for Crystal Structure Resolution. University of Göttingen, Göttingen, Germany., (1997).
- [15] G.M. Sheldrick, Crystal structure refinement with SHELXL, *Acta Crystallogr. Sect. C Struct. Chem.* 71 (2015) 3–8. doi:10.1107/S2053229614024218.
- [16] L.J. Farrugia, WinGX and ORTEP for Windows: An update, *J. Appl. Crystallogr.* 45 (2012) 849–854. doi:10.1107/S0021889812029111.
- [17] K. Brandsburg, Programa de representação de estruturas cristalinas, Diam. Versão 2.1.c. Programa Represent. Estruturas Cristal. (n.d.).
- [18] C. and L.S. Institute, Clinical & Laboratory Standards Institute: CLSI Guidelines, (2012).
- [19] L.F. Leandro, M.J.O. Cardoso, S.D.C. Silva, M.G.M. Souza, R.C.S. Veneziani, S.R. Ambrosio, C.H.G. Martins, Antibacterial activity of *Pinus elliottii* and its major compound, dehydroabiatic acid, against multidrug-resistant strains, *J. Med. Microbiol.* 63 (2014) 1649–1653. doi:10.1099/jmm.0.081711-0.
- [20] Clinical and Laboratory Standards Institute, Clinical & Laboratory Standards Institute: CLSI Guidelines, (2008).

- [21] K.D. Goughenour, J.M. Balada-Llasat, C.A. Rappleye, Quantitative microplate-based growth assay for determination of antifungal susceptibility of *histoplasma capsulatum* yeasts, *J. Clin. Microbiol.* 53 (2015) 3286–3295.
doi:10.1128/JCM.00795-15.
- [22] R. Takjoo, R. Centore, L. Rhyman, P. Ramasami, Nickel(II) and copper(II) complexes of allyl 2-(thiophen-2-ylmethylene)hydrazinecarbodithioate: synthesis, X-ray crystal structures, and theoretical study., *J. Coord. Chem.* 65 (2012) 1569–1579. <http://10.0.4.56/00958972.2012.675058>.
- [23] N. Nanjundan, R. Narayanasamy, S. Geib, K. Velmurugan, R. Nandhakumar, M.D. Balakumaran, P.T. Kalaichelvan, Distorted tetrahedral bis-(N,S) bidentate Schiff base complexes of Ni(II), Cu(II) and Zn(II): Synthesis, characterization and biological studies, *Polyhedron.* 110 (2016) 203–220.
doi:<https://doi.org/10.1016/j.poly.2016.02.049>.
- [24] R. Takjoo, R. Centore, Synthesis, X-ray structure, spectroscopic properties and DFT studies of some dithiocarbazate complexes of nickel(II), *J. Mol. Struct.* 1031 (2013) 180–185. doi:<https://doi.org/10.1016/j.molstruc.2012.07.018>.
- [25] E. Zangrando, M.S. Begum, M.C. Sheikh, R. Miyatake, M.M. Hossain, M.M. Alam, M.A. Hasnat, M.A. Halim, S. Ahmed, M.N. Rahman, A. Ghosh, Synthesis, characterization, density functional study and antimicrobial evaluation of a series of bischelated complexes with a dithiocarbazate Schiff base ligand, *Arab. J. Chem.* 10 (2017) 172–184.
doi:<https://doi.org/10.1016/j.arabjc.2016.07.019>.
- [26] N. Nanjundan, R. Narayanasamy, R.J. Butcher, J.P. Jasinski, K. Velmurugan, R. Nandhakumar, M.D. Balakumaran, P.T. Kalaichelvan, V.G. Gnanasoundari, Synthesis, crystal structure, biomolecular interactions and anticancer properties

- of Ni(II), Cu(II) and Zn(II) complexes bearing S-allyldithiocarbazate, *Inorganica Chim. Acta.* 455, Part (2017) 283–297.
doi:<https://doi.org/10.1016/j.ica.2016.10.035>.
- [27] C. Deckert, D. Bittner, L.M. Carrella, D. Schollmeyer, E. Rentschler, *Synthesis, Structural and Spectroscopic Characterization of Cr III , Fe III , Co III , Ni II and Cu II Complexes with an Asymmetric 1,3,4-Thiadiazole Ligand*, *Eur. J. Inorg. Chem.* (2016) 1738–1747. doi:10.1002/ejic.201501400.
- [28] R. Takjoo, R. Centore, S.S. Hayatolghheibi, *Mixed ligand complexes of cadmium(II) and copper(II) dithiocarbazate: Synthesis, spectral characterization, X-ray crystal structure*, *Inorganica Chim. Acta.* 471 (2018) 587–594.
doi:<https://doi.org/10.1016/j.ica.2017.11.043>.
- [29] M.A.A.A. Islam, M.C. Sheikh, M.H. Islam, R. Miyatake, E. Zangrando, *Crystal structure of 1,2-bis((benzylsulfanyl){2-[1-(2-hydroxyphenyl)ethylidene]hydrazin-1-ylidene}methyl)disulfane*, *Acta Crystallogr. Sect. E Crystallogr. Commun.* 72 (2016) 337–339.
doi:10.1107/S2056989016002371.
- [30] M.A. Ali, A.H. Mirza, W.Y. Ting, M.H.S.A. Hamid, P. V Bernhardt, R.J. Butcher, *Mixed-ligand nickel(II) and copper(II) complexes of tridentate ONS and NNS ligands derived from S-alkyldithiocarbazates with the saccharinate ion as a co-ligand*, *Polyhedron.* 48 (2012) 167–173.
doi:<https://doi.org/10.1016/j.poly.2012.08.069>.
- [31] C.C. Gatto, P.M. Miguel, C.M. Almeida, P.H.O. Santiago, C.R.K. Paier, C. Pessoa, *A copper(II) complex of a semicarbazone: crystal structure, spectroscopic analysis and cytotoxicity against human cancer cell lines*, *Transit. Met. Chem.* 42 (2017) 503–508. doi:10.1007/s11243-017-0154-8.

- [32] S.J. Li, K. Li, X.Y. Qiu, X.J. Yao, Two new isomeric di- μ -oxo bis[oxovanadium(V)] complexes containing schiff base ligands, *J. Chem. Crystallogr.* 42 (2012) 879–883. doi:10.1007/s10870-012-0330-9.
- [33] X.-Y. Qiu, C. Zhang, S.-Z. Li, G.-X. Cao, P. Qu, F.-Q. Zhang, J.-G. Ma, B. Zhai, Synthesis, crystal structures and cytotoxic activity of mononuclear nickel(II) and dinuclear zinc(II) complexes with ligand derived from S-benzylthiocarbamate, *Inorg. Chem. Commun.* 46 (2014) 202–206. doi:https://doi.org/10.1016/j.inoche.2014.05.015.
- [34] E.C. Alyea, M.C. Jennings, C.H.N. S, Structural S-Benzylthiocarbamate N-Oxide and Its Dimeric Copper @ Nitrate Complex, (1991) 1625–1629. doi:https://doi.org/10.1016/S0277-5387(00)83773-0.
- [35] M.A.-A.A.A. Islam, M.C. Sheikh, M.S. Alam, E. Zangrando, M.A. Alam, M.T.H. Tarafder, R. Miyatake, Synthesis, characterization and bio-activity of a bidentate NS Schiff base of S-allylthiocarbamate and its divalent metal complexes: X-ray crystal structures of the free ligand and its nickel(II) complex, *Transit. Met. Chem.* 39 (2014) 141–149. doi:10.1007/s11243-013-9783-8.
- [36] A. Taha, A.A.A. Emara, M.M. Mashaly, O.M.I. Adly, Spectral characterization, molecular modeling and antimicrobial studies on hydrazone metal complexes of 5-acetyl-4-hydroxy-2H-1,3-thiazine-2,6(3H)dione and S-methyl dithiocarbamate, *Spectrochim. Acta - Part A Mol. Biomol. Spectrosc.* 130 (2014) 429–439. doi:10.1016/j.saa.2014.04.007.
- [37] M. Yazdanbakhsh, R. Takjoo, Synthesis, crystal structure of new linear trinuclear isovalence Co(II)([Co₃(H-L)₂(L)₂]), and visualizing intermolecular interactions with Hirshfeld surface method, *Struct. Chem.* 19 (2008) 895–903. doi:10.1007/s11224-008-9356-1.

- [38] W.J. Geary, The use of conductivity measurements in organic solvents for the characterisation of coordination compounds, *Coord. Chem. Rev.* 7 (1971) 81–122. doi:10.1016/S0010-8545(00)80009-0.
- [39] N. Bharti, F. Athar, M.R. Maurya, A. Azam, Synthesis, characterization and in vitro anti-amoebic activity of new palladium(II) complexes with 5-nitrothiophene-2-carboxaldehyde N(4)-substituted thiosemicarbazones, *Bioorg. Med. Chem.* 12 (2004) 4679–4684.
doi:https://doi.org/10.1016/j.bmc.2004.06.036.
- [40] M.X. Li, L.Z. Zhang, C.L. Chen, J.Y. Niu, B.S. Ji, Synthesis, crystal structures, and biological evaluation of Cu(II) and Zn(II) complexes of 2-benzoylpyridine Schiff bases derived from S-methyl- and S-phenyldithiocarbazates, *J. Inorg. Biochem.* 106 (2012) 117–125.
doi:https://doi.org/10.1016/j.jinorgbio.2011.09.034.

Figure Captions

Figure 1. Molecular structures of H_2L^1 with crystallographic labelling (30% probability displacement ellipsoids). Intramolecular hydrogen bonds are shown as dashed lines.

Figure 2. Molecular structures of **(1)** and **(2)** with crystallographic labelling (30% probability displacement ellipsoids).

Figure 3. UV-vis absorption spectra of the ligands and copper(II) derivatives in MeOH and DMF (concentration 20 μM).

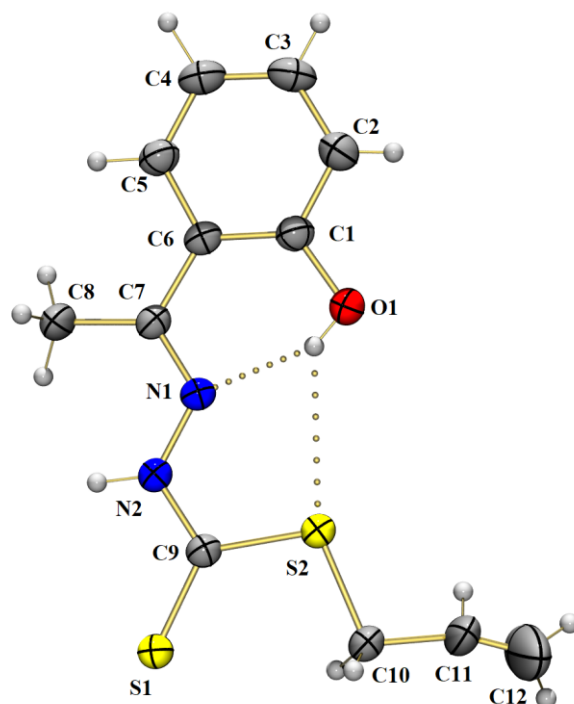
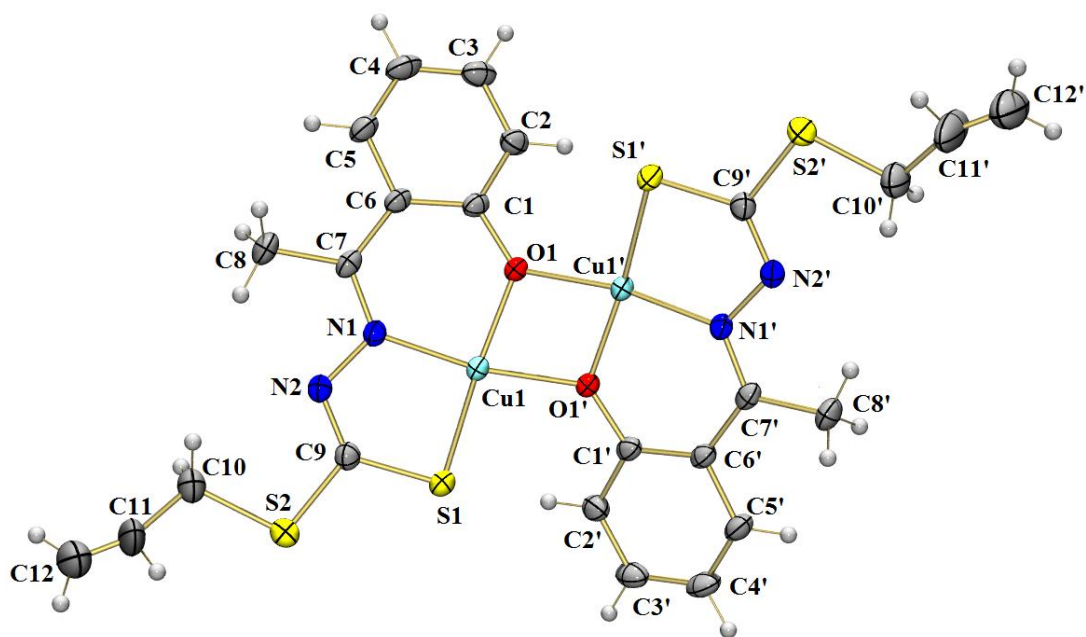
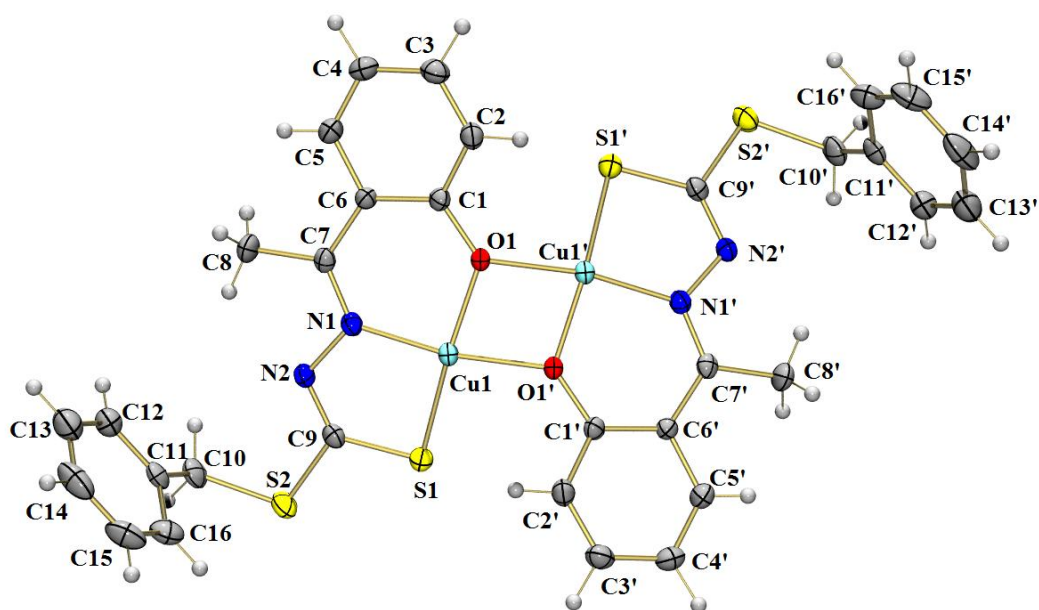


Figure 1. Molecular structures of H_2L^1 with crystallographic labelling (30 % probability displacement ellipsoids). Intramolecular hydrogen bonds are shown as dashed lines.



(1)



(2)

Figure 2. Molecular structures of (1) and (2) with crystallographic labelling (30% probability displacement ellipsoids).

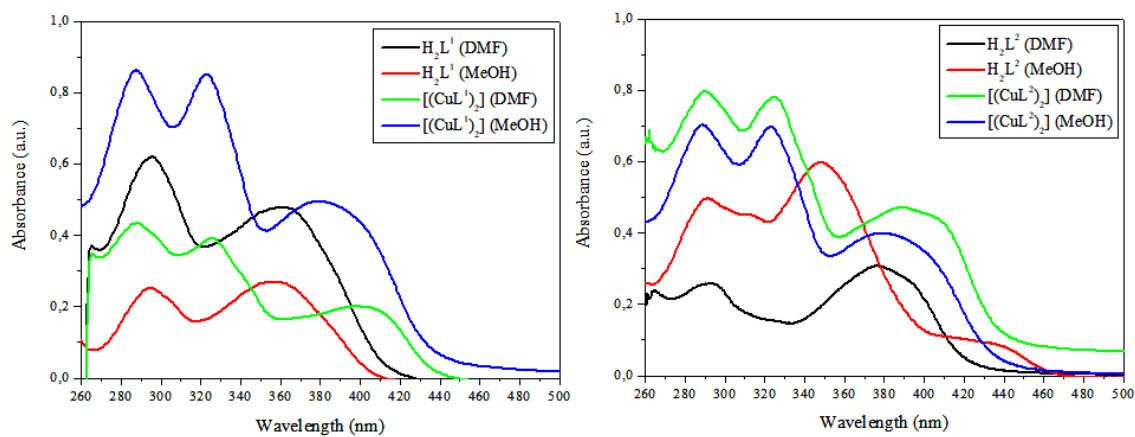


Figure 3. UV-vis absorption spectra of the ligands and copper(II) derivatives in MeOH and DMF (concentration 20 μ M).

Tables

Table 1. X-ray diffraction data collection and refinement parameters for H_2L^1 , 1 and 2.

Table 2. Selected bond distances (\AA) and bond angles ($^\circ$) for the ligand H_2L^1 and the complexes (1) and (2).

Table 3. UV–vis data (in different solvents) of the ligands and copper(II) derivatives.

Table 4. Minimal inhibitory concentration ($\mu\text{g.mL}^{-1}$) of H_2L^1 , H_2L^2 and the complexes (1) and (2) against the multiresistant bacteria.

Table 5. Minimal inhibitory concentration ($\mu\text{g.mL}^{-1}$) of H_2L^1 , H_2L^2 and the complexes (1) and (2) against the yeasts.

Table 1. X-ray diffraction data collection and refinement parameters for H₂L¹, 1 and 2.

	H ₂ L ¹	(1)	(2)
Chemical formula	C ₁₂ H ₁₄ N ₂ OS ₂	C ₁₂ H ₁₂ CuN ₂ OS ₂	C ₁₆ H ₁₄ CuN ₂ OS ₂
M (g mol ⁻¹)	266.37	327.90	377.95
Crystal system	Triclinic	Monoclinic	Monoclinic
Space group	<i>P</i> -1	<i>C</i> 2/ <i>c</i>	<i>C</i> 2/ <i>c</i>
Unit cell <i>a</i> (Å)	5.382(3)	26.031(13)	31.407(12)
<i>b</i> (Å)	8.429(4)	7.447(4)	7.318(3)
<i>c</i> (Å)	15.186(7)	13.539(6)	13.48(5)
α (°)	88.200(3)	90	90
β (°)	83.616(2)	96.051(3)	98.689(2)
γ (°)	78.528(3)	90	90
<i>V</i> (Å ³)	670.86(6)	2610.2(2)	3061.3(2)
<i>Z</i>	2	8	8
<i>D</i> _c /g cm ⁻³	1.319	1.669	1.640
Index ranges	-7 ≤ <i>h</i> ≤ 7	-30 ≤ <i>h</i> ≤ 32	-39 ≤ <i>h</i> ≤ 31
	-11 ≤ <i>k</i> ≤ 11	-9 ≤ <i>k</i> ≤ 9	-9 ≤ <i>k</i> ≤ 8
	-19 ≤ <i>l</i> ≤ 20	-16 ≤ <i>l</i> ≤ 16	-16 ≤ <i>l</i> ≤ 16
Absorption coefficient /mm ⁻¹	0.382	1.980	1.701
Absorption correction	multi-scan	multi-scan	multi-scan
Max/min transmission	0.949 / 0.748	0.758 / 0.522	0.955 / 0.712
Measured reflections	13994	11535	14026
Independent reflections / <i>R</i> _{int}	3256 / 0.029	2693 / 0.0368	3153 / 0.0773
Refined parameters	196	181	216
<i>R</i> 1 (<i>F</i>) / <i>wR</i> 2 (<i>F</i> ²) (<i>I</i> > 2σ(<i>I</i>))	0.0435 / 0.1142	0.0322 / 0.0806	0.0486 / 0.0886
GooF	1.109	1.064	1.055
Largest diff. peak and hole (eÅ ⁻³)	0.205 and -0.296	0.338 and -0.294	0.620 and -0.452

Table 2. Selected bond distances (Å) and bond angles (°) for the ligand H₂L¹ and the complexes (1) and (2).

	H ₂ L ¹	(1)	(2)
C(1)–O(1)	1.354(3)	1.353(3)	1.354(4)
C(7)–N(1)	1.297(3)	1.308(3)	1.304(5)
N(1)–N(2)	1.372(3)	1.398(3)	1.409(4)
N(2)–C(9)	1.353(3)	1.284(3)	1.286(5)
C(9)–S(1)	1.659(2)	1.728(3)	1.728(4)
C(9)–S(2)	1.734(2)	1.746(3)	1.750(4)
S(2)–C(10)	1.814(2)	1.810(3)	1.810(3)
Cu(1)–O(1)	-	1.908(18)	1.911(3)
Cu(1)–O(1) ^(a)	-	1.992(18)	2.005(3)
Cu(1)–N(1)	-	1.940(2)	1.935(3)
Cu(1)–S(1)	-	2.199(3)	2.201(13)
Cu(1)–Cu(1)	-	2.926(6)	2.966(10)
C(7)–N(1)–N(2)	120.08(18)	115.20(2)	114.70(3)
N(1)–N(2)–C(9)	119.09(18)	113.90(2)	113.50(3)
N(2)–C(9)–S(1)	113.35(16)	127.50(2)	127.30(2)
S(1)–C(9)–S(2)	125.34(12)	113.43(16)	112.70(2)
N(2)–C(9)–S(2)	121.31(16)	119.10(2)	120.0(3)
C(1)–O(1)–Cu(1)	-	127.23(17)	127.30(3)
C(1)–O(1)–Cu(1) ^(a)	-	131.68(17)	131.0(3)
O(1)–Cu(1)–N(1)	-	93.49(9)	93.75(13)
N(1)–Cu(1)–O(1) ^(a)	-	169.51(14)	170.25(13)
N(1)–Cu(1)–S(1)	-	88.93(7)	88.62(11)
S(1)–Cu(1)–O(1)	-	170.53(7)	170.55(9)
S(1)–Cu(1)–O(1) ^(a)	-	100.32(6)	100.55(9)
O(1)–Cu(1)–O(1) ^(a)	-	76.60(9)	76.67(12)
Cu(1)–O1–Cu(1) ^(a)	-	97.23(8)	98.44(12)

^(a) Symmetry operation: complex (1): -x, -y, -z - 1/2 and complex (2) -x, -y, -z + 1/2.

Table 3. UV–vis data (in different solvents) of the ligands and copper(II) derivatives.

		$\pi \rightarrow \pi^*$ ^a	log ϵ	$n \rightarrow \pi^*$ ^a	log ϵ	LMCT ^a	log ϵ
H₂L¹	DMF	294	4.49	361	4.38	-	-
	MeOH	293	4.09	358	4.13	-	-
H₂L²	DMF	292	4.11	376	4.18	-	-
	MeOH	290	4.39	348	4.47	-	-
(1)	DMF	287	4.63	324	4.29	405	4.00
	MeOH	287	4.33	322	4.63	382	4.39
(2)	DMF	289	4.59	324	4.59	395	4.36
	MeOH	288	4.54	322	4.53	380	4.30

(a) Absorption band values in nm.

Table 4. Minimal inhibitory concentration ($\mu\text{g mL}^{-1}$) of H_2L^1 , H_2L^2 and the complexes (1) and (2) against the multiresistant bacteria.

Bacterial strains	H_2L^1	H_2L^2	$\text{Cu}(\text{CH}_3\text{COO})_2$	(1)	(2)	Tetracycline
Gram-positive						
<i>Enterococcus faecalis</i> NCTC 775	>400	400	>400	12.5	6.25	-
<i>Enterococcus faecalis</i> Clinical Isolate	>400	>400	>400	400	25	-
<i>Enterococcus faecium</i> NCTC 7171	>400	>400	>400	6.25	12.5	-
<i>Staphylococcus epidermidis</i> ATCC 14990	400	400	>400	6.25	6.25	-
<i>Staphylococcus epidermidis</i> Clinical Isolate	400	>400	>400	3.12	6.25	-
<i>Staphylococcus aureus</i> ATCC 29213	100	400	>400	1.56	3.12	-
<i>Staphylococcus aureus</i> Clinical Isolate	100	>400	>400	>400	>400	-
<i>Staphylococcus capitis</i> ATCC 27840	50	400	>400	3.12	6.25	-
Gram-negative						
<i>Pseudomonas aeruginosa</i> Clinical Isolate	400	400	>400	>400	>400	-
<i>Enterobacter cloacae</i> Clinical Isolate	>400	>400	>400	>400	400	-
<i>Klebsiella pneumoniae</i> Clinical Isolate	>400	>400	>400	>400	>400	-
Positive Control						
<i>Staphylococcus aureus</i>	-	-	-	-	-	0.37

ATCC 29213							
<i>Escherichia coli</i>	-	-	-	-	-	-	0.73
ATCC 25922							
Negative Control							
DMSO*	-	-	-	-	-	-	-

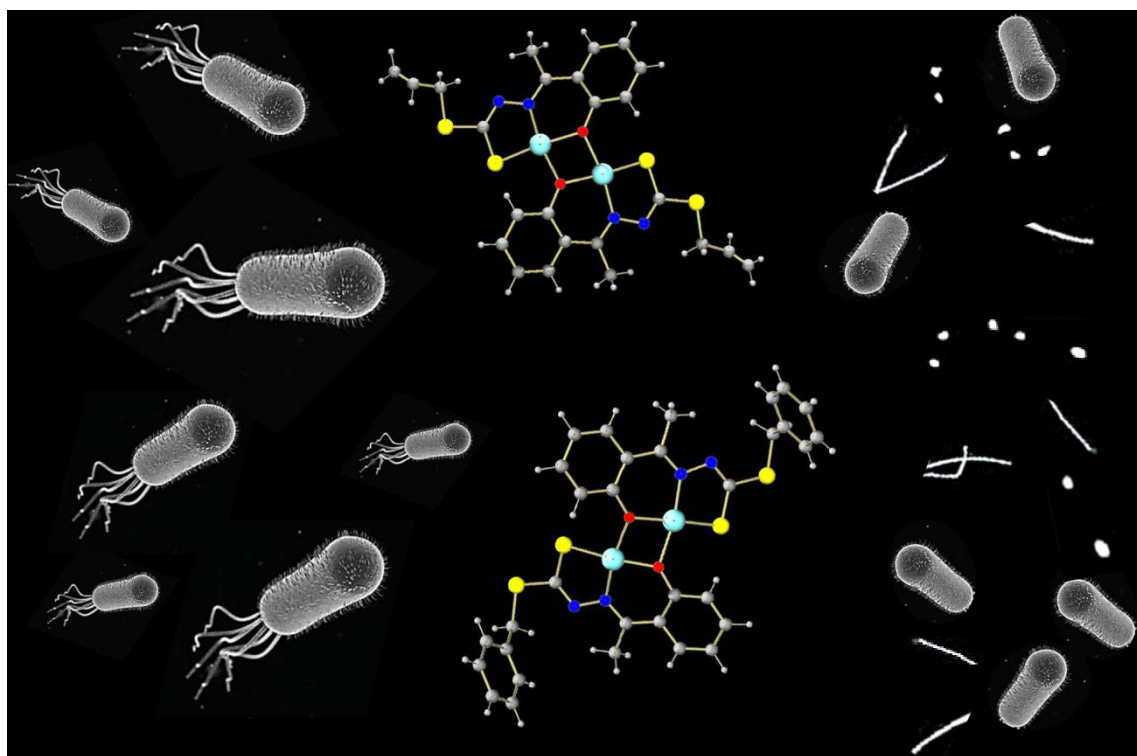
Concentrations of the samples evaluated against the bacteria = 0.195 $\mu\text{g.mL}^{-1}$ to 400 $\mu\text{g.mL}^{-1}$. (-) : Not determined. DMSO* – Dimethylsulfoxide: not influenced in microbial growth.

Table 5. Minimal inhibitory concentration ($\mu\text{g.mL}^{-1}$) of H_2L^1 , H_2L^2 and the complexes (1) and (2) against the yeasts.

Yeasts	H_2L^1	H_2L^2	$\text{Cu}(\text{CH}_3\text{COO})_2$	(1)	(2)	Amphotericin B
<i>Candida albicans</i> ATCC 28366	>3000	>3000	>3000	1500	750	-
<i>Candida glabrata</i> ATCC 15126	>3000	>3000	>3000	375	375	-
<i>Candida tropicalis</i> ATCC 13803	3000	3000	>3000	375	750	-
Positive Control						
<i>Candida parapsilosis</i> ATCC 22019	-	-	-	-	-	0.5
<i>Candida krusei</i> ATCC 6258	-	-	-	-	-	1.0
Negative Control						
DMSO*	-	-	-	-	-	-

Concentrations of the samples evaluated against yeasts = 1.46 $\mu\text{g.mL}^{-1}$ to 3000 $\mu\text{g.mL}^{-1}$. (-): Not determined. DMSO* – Dimethylsulfoxide: not influenced in microbial growth.

Graphical abstract



ACCEPTED

Highlights

- Dimeric Cu(II) complexes and dithiocarbamate ligands were successfully synthesized.
- Molecular structures of S-allyl-2-(2-hydroxyphenyl-ethylidene)dithiocarbamate ligand and of the complexes $[(CuL^1)_2]$ and $[(CuL^2)_2]$ were confirmed by single crystal X-ray diffraction experiment.
- Tests of the antibacterial and antifungal properties against several multiresistant bacteria and fungi were performed.